nature biotechnology

Single-molecule enzyme-linked immunosorbent assay detects serum proteins at subfemtomolar concentrations

David M Rissin[1,3], Cheuk W Kan[1,3], Todd G Campbell[1], Stuart C Howes[1], David R Fournier[1], Linan Song[1], Tomasz Piech[1], Purvish P Patel[1], Lei Chang[1], Andrew J Rivnak[1], Evan P Ferrell[1], Jeffrey D Randall[1], Gail K Provuncher[1], David R Walt[2] & David C Duffy[1]

© 2010 Nature America, Inc. All rights reserved.

The ability to detect single protein molecules[1,2] in blood could accelerate the discovery and use of more sensitive diagnostic biomarkers. To detect low-abundance proteins in blood, we captured them on microscopic beads decorated with specific antibodies and then labeled the immunocomplexes (one or zero labeled target protein molecules per bead) with an enzymatic reporter capable of generating a fluorescent product. After isolating the beads in 50-fl reaction chambers designed to hold only a single bead, we used fluorescence imaging to detect single protein molecules. Our single-molecule enzyme-linked immunosorbent assay (digital ELISA) approach detected as few as ~10–20 enzyme-labeled complexes in 100 μl of sample (~10^{-19} M) and routinely allowed detection of clinically relevant proteins in serum at concentrations (<10^{-15} M) much lower than conventional ELISA[3–5]. Digital ELISA detected prostate-specific antigen (PSA) in sera from patients who had undergone radical prostatectomy at concentrations as low as 14 fg/ml (0.4 fM).

The clinical use of protein biomarkers to differentiate between healthy and disease states, and to monitor disease progression, requires the measurement of low concentrations of proteins in complex samples. Current immunoassays typically measure proteins at concentrations above 10^{-12} M[6]. The serum concentrations of the majority of proteins important in cancer[7], neurological disorders[8,9] and the early stages of infection[10], however, are thought to range from 10^{-16} to 10^{-12} M. For instance, a 1-mm^3 tumor composed of a million cells that each secrete 5,000 proteins into 5 liters of circulating blood translates to a concentration of ~2×10^{-15} M (or 2 fM). Moreover, serum from individuals recently infected with HIV contains 10–3,000 virions per ml, resulting in estimated concentrations of the p24 capsid antigen ranging from 50×10^{-18} M (50 aM) to 15×10^{-15} M (15 fM)[10]. Attempts to develop methods capable of measuring these concentrations of proteins have focused on the replication of nucleic acid labels on proteins[11,12], or on measuring the bulk, ensemble properties of labeled protein molecules[13–16]. The work of Mirkin *et al.*[12,17] and others[18] using labels based on gold nanoparticles and DNA biobarcodes has pushed the detection of proteins into the low femtomolar range; a recent report using this technology demonstrated the detection of 10 fM of PSA in serum[17]. Nonetheless, the sensitivities achieved by methods for detecting proteins still lag behind those for nucleic acids, such as PCR, limiting the number of gene products that have been detected in blood[6,19]. The isolation and detection of single protein molecules provides a promising approach for measuring extremely low concentrations of proteins[1,2]. For example, Todd *et al.*[2] have developed flow-based methods for serially detecting single fluorescently labeled detection antibodies that have been released from immunocomplexes formed on solid substrates. Here we report an approach for detecting thousands of single protein molecules simultaneously using the same reagents as the gold standard for detecting proteins, namely, the ELISA. This method has been used to detect proteins in serum at subfemtomolar concentrations.

Our approach makes use of arrays of femtoliter-sized reaction chambers (**Fig. 1**)—which we term single-molecule arrays (SiMoAs)—that can isolate and detect single enzyme molecules[20–24]. This approach builds from the work of Walt *et al.*[20–23], who used these arrays to study the kinetics[21] and inhibition[20] of single enzymes. Our objective was to exploit the ability of SiMoAs to trap and detect single enzymes to detect single enzyme–labeled proteins. In the first step of this single-molecule immunoassay (**Fig. 1a**), a sandwich antibody complex is formed on microscopic beads (2.7 μm diameter), and the bound complexes are labeled with an enzyme, as in a conventional bead-based ELISA. When assaying samples containing extremely low concentrations of protein, the ratio of protein molecules (and the resulting enzyme-labeled complex) to beads is small (typically <1:1) and, as such, the percentage of beads that contain a labeled immunocomplex follows a Poisson distribution. At low concentrations of protein, the Poisson distribution indicates that beads carry either a single immunocomplex or none. For example, if 50 aM of a protein in 0.1 ml (3,000 molecules) is captured and labeled on 200,000 beads, then 1.5% of the beads will carry one protein molecule and 98.5% will not carry any protein molecules (**Fig. 1b**)[22]. It is not possible to detect these low numbers of enzyme labels using standard detection technology (for example, a plate reader), because the fluorophores generated by each enzyme diffuse into a large assay volume (typically 0.1–1 ml), and it takes hundreds of thousands of enzyme labels to generate a

[1]Quanterix Corporation, Cambridge, Massachusetts, USA. [2]Department of Chemistry, Tufts University, Medford, Massachusetts, USA. [3]These authors contributed equally to this work. Correspondence should be addressed to D.C.D. (dduffy@quanterix.com).

Received 1 February; accepted 29 April; published online 23 May 2010; doi:10.1038/nbt.1641

Fujirebio Diagnostics, Inc. v. Quanterix Corp.
EX-1005
000001

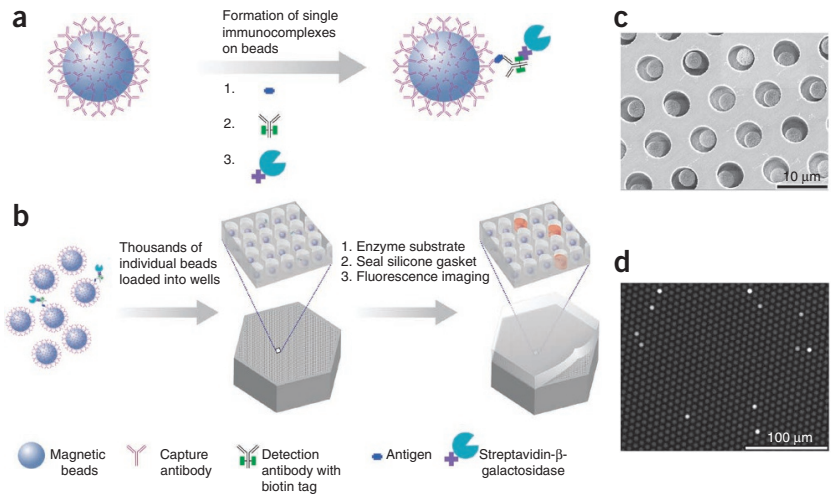


Figure 1 Digital ELISA based on arrays of femtoliter-sized wells. (**a**,**b**) Single protein molecules are captured and labeled on beads using standard ELISA reagents (**a**), and beads with or without a labeled immunoconjugate are loaded into femtoliter-volume well arrays for isolation and detection of single molecules by fluorescence imaging (**b**). (**c**) Scanning electron micrograph of a small section of a femtoliter-volume well array after bead loading. Beads (2.7 µm diameter) were loaded into an array of wells with diameters of 4.5 µm and depths of 3.25 µm. (**d**) Fluorescence image of a small section of the femtoliter-volume well array after signals from single enzymes are generated. Whereas the majority of femtoliter-volume chambers contain a bead from the assay, only a fraction of those beads possess catalytic enzyme activity, indicating a single, bound protein molecule. The concentration of protein in bulk solution is correlated to the percentage of beads that carry a protein molecule.

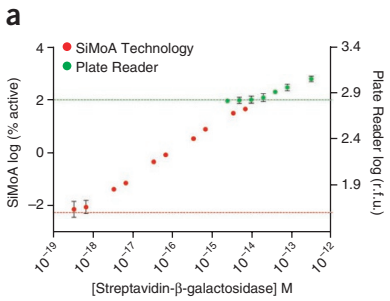
© 2010 Nature America, Inc. All rights reserved.

fluorescence signal above background. In contrast, SiMoAs permit the detection of very low concentrations of enzyme labels by confining the fluorophores generated by individual enzymes to extremely small volumes (~50 fl), ensuring a high local concentration of fluorescent product molecules. To achieve this confinement in our assay, beads are loaded into an array of femtoliter-sized wells; we used 2-mm-wide arrays with ~50,000 wells, each with a diameter of 4.5 µm and a depth of 3.25 µm (**Fig. 1c**). After sealing the loaded arrays against a rubber gasket in the presence of a droplet of fluorogenic enzyme substrate, each bead is isolated in a femtoliter-volume reaction chamber. Beads possessing a single enzyme–labeled immunocomplex generate a high concentration of fluorescent product that is restricted to the 50-fl reaction chamber (**Fig. 1d**). By acquiring time-lapsed fluorescence images of the array using standard microscope optics, it is possible to distinguish beads associated with a single enzyme molecule ("on" well) from those not associated with an enzyme ("off" well); **Supplementary Figure 1** shows histograms of fluorescence from "on" and "off" wells. Imaging the arrays allows simultaneous detection of tens to tens of thousands of single immunocomplexes. The protein concentration in the test sample is determined by counting the number of wells containing both a bead and fluorescent product relative to the total number of wells containing beads (**Fig. 1d**). As SiMoAs enable concentration to be determined digitally rather than by using the total analog signal, we call our approach to detecting single immunocomplexes digital ELISA.

We first assessed the intrinsic sensitivity of this strategy by creating populations of beads with well-characterized enzyme-to-bead ratios. We mixed 400,000 biotin-modified beads with a range of concentrations of the enzyme conjugate streptavidin-β-galactosidase (SβG). For convenience, biotinylated beads were provided by hybridizing biotinylated DNA with beads functionalized with complementary DNA. (We note that this experiment should not be construed as a sensitive DNA assay; the sensitivity of such an assay is limited by nonspecific interactions between the enzyme conjugate and surface-bound DNA as shown in **Supplementary Fig. 2**.) These beads were detected in two different ways. First, we assayed an ensemble of beads in 100 µl using a fluorescence plate reader after 1 h incubation with 100 µM resorufin-β-D-galactopyranoside (RGP), a fluorogenic substrate for β-galactosidase. The detection limit for enzyme on the plate reader was 15 fM of SβG (**Fig. 2**). Second, we loaded the beads into femtoliter-volume well arrays and, after sealing a solution of RGP into the wells of the array, allowed the signal from single enzymes to accumulate in the reaction chambers for 2.5 min, acquiring fluorescent images every 30 s. At the end of the experiment we used an image of the array that was acquired in white light to identify wells that contained beads (bead-containing wells scatter light differently than empty wells). The fluorescent images were used to determine which of those beads had an associated bound enzyme (from increasing intensity in time-lapsed fluorescent images). **Figure 2** shows a log-log plot of the percentage of beads that contained an enzyme as a function of bulk SβG concentration. The lowest concentration of enzyme conjugate detected was 350 zeptomolar (zM) and the calculated limit of detection (LOD)—determined by extrapolating the enzyme concentration at a signal equal to background plus 3 s.d. of the background signal—was 220 zM. The sensitivity of SiMoAs to intrinsic label was, therefore, ~10–20 enzymes in 100 µl, corresponding to an increase in sensitivity over ensemble measurements using a typical ELISA-plate reader of a factor of about 68,000. For comparison, chemiluminescent detection of alkaline phosphatase[4], a highly sensitive enzyme reporter system widely used in clinical diagnostics, has an LOD of about 30 aM (see <http://www.turnerbiosystems.com/doc/appnotes/S_0096.php>). The high sensitivity that arises from the thermodynamic and kinetic efficiency of the capture and detection processes in our approach are discussed below and detailed in **Supplementary Table 1**.

The linear dynamic range of digital detection of enzyme labels by SiMoAs is determined by the ability to distinguish "on" and "off" wells. At ratios of enzyme to beads of less than ~1:10, Poisson statistics show that the only statistically significant populations of beads are those carrying either one enzyme or no enzyme. Single enzymes can be detected provided that sufficient beads are interrogated and the number of active beads rises above the Poisson noise of counting active beads. At ratios of enzyme to beads greater than ~1:10, the fraction of active beads becomes much higher, and Poisson statistics show that there are a significant number of beads with multiple enzymes. To quantify the number of detected enzymes and maintain linearity in the subpopulations of beads with multiple enzymes, we use Poisson statistics to convert the number of active beads to the number of detected enzymes (see **Supplementary Table 1**). As the percentage of active beads approaches 50% (ratios of enzyme to beads greater than ~1:1.5), however, distinguishing "on" and "off" wells using image analysis software becomes challenging, and we reach a practical upper limit of the digital dynamic range. For example, the

Fujirebio Diagnostics, Inc. v. Quanterix Corp.
EX-1005
000002



b

[SβG] (aM)	Average number of active beads	Average fraction of active beads	Measurement CV	Poisson Noise CV
0	1	0.0016%	87%	122%
0.35	3	0.0086%	75%	55%
0.7	5	0.0099%	63%	46%
3.5	22	0.0413%	10%	21%
7	38	0.0713%	15%	16%
35	237	0.4461%	1%	7%
70	385	0.8183%	5%	5%
350	1787	3.3802%	2%	2%
700	4036	7.5865%	5%	2%
3500	15634	30.6479%	3%	1%
7000	24836	44.5296%	1%	1%

Figure 2 Digitization of enzyme-linked complexes greatly increases sensitivity compared with bulk, ensemble measurements. (**a**) Log-log plot of signal output (% active beads for single-molecule array (SiMoA) or relative fluorescence units (r.f.u.) for plate reader) as a function of the concentration of streptavidin-β-galactosidase (SβG) captured on biotinylated beads. SβG concentrations for the ensemble readout ranged from 3 fM to 300 fM, with a detection limit of 15×10^{-15} M (15 fM; green broken line). For the SiMoA assay, SβG concentrations ranged from 350 zM to 7 fM, demonstrating a linear response of ~10,000-fold, with a calculated detection limit of 220×10^{-21} M (220 zM; red broken line). Error bars are based on the s.d. over three replicates for both technologies. LODs were determined by extrapolating the concentration from the signal equal to background signal plus 3 s.d. of the background signal. (**b**) The imprecision from SiMoAs is determined by the Poisson noise of counting single events. The intrinsic variation (Poisson noise) of counting single active beads is given by $\sqrt{n}$. Comparing the Poisson noise–associated coefficient of variation (%CV = $\sqrt{n}/n$) with the SiMoA %CV over three measurements confirmed that the imprecision of the assay is determined by counting error.

© 2010 Nature America, Inc. All rights reserved.

signal at 7 fM (~45% active) in **Figure 2** deviates from linearity. As a result, the digital, linear dynamic range demonstrated here using 50,000 wells spanned approximately four orders of magnitude (from 3.5 fM down to 350 zM). Provided that proteins are labeled using appropriate enzyme concentrations (see below), this dynamic range is sufficient for many clinical applications.

We have developed digital ELISAs for two clinically relevant proteins—PSA and tumor necrosis factor-α (TNF-α)—to determine the sensitivity of the approach for detecting proteins in blood. The critical parameters in developing these assays were the concentrations of the beads and the two labeling reagents (detection antibody and enzyme conjugate). The choice of bead concentration depends on several competing factors. First, a sufficient number of beads must be present to capture most of the target analyte from thermodynamic and kinetic perspectives. Thermodynamically, 200,000 beads in 100 µl, each of which has ~80,000 antibodies[25] bound to it, equates to an antibody concentration of about 0.3 nM. The antibody-protein equilibrium at that concentration permits a high capture efficiency (>70%) (D.M.R., E.P.F., D.C.D., unpublished work). Kinetically, for 200,000 beads dispersed in 100 µl, the average distance between beads is about 80 µm. Proteins the size of TNF-α and PSA (17.3 and 30 kDa, respectively) will diffuse 80 µm in <1 min, suggesting that capture of the protein molecules will not be limited kinetically over a 2-h incubation. Second, a sufficient number of beads must be present to be loaded onto the arrays to limit Poisson noise. Loading 200,000 beads into 50,000-well arrays typically results in 20,000–30,000 beads being trapped in femtoliter-sized wells. For a typical background signal of 1% active beads (see below), this loading results in a background signal of 200–300 active beads detected, corresponding to an acceptable coefficient of variation (CV) from Poisson noise of 6–7%. Third, excessive bead concentrations can lead to both increases in nonspecific binding that reduces signal-to-background and low ratios of analyte to beads that can result in high CVs from Poisson noise. The balance of these factors means that 200,000 to 1,000,000 beads per 100 µl of test sample is optimal for digital ELISA. The concentrations of detection antibody and enzyme conjugate were also minimized to yield the acceptable background signal (1%) and Poisson noise (**Supplementary Discussion**).

Figure 3 shows data from digital ELISAs for PSA and TNF-α. The human forms of the proteins were spiked into 25% bovine serum to final concentrations representative of clinical test samples. A fourfold dilution factor is typically used to reduce matrix effects in immunoassays[4]. Using digital ELISA to detect PSA in 25% serum, we obtained an LOD of ~50 aM (1.5 fg/ml), which equates to an LOD in whole serum of ~200 aM (6 fg/ml). The lowest concentration tested and detected was 250 aM in 25% serum, corresponding to 1 fM in whole serum. As LOD is determined by extrapolating the concentration at background plus 3 s.d. of the background, LODs for different runs are dependent on the CV of the background. We obtained subfemtomolar LODs of PSA in whole serum over several experiments with typical background variances. For comparison, a leading commercial PSA assay (ADVIA Centaur, Siemens) reports an LOD of 3 pM (0.1 ng/ml) in human serum, and ultrasensitive assays have been reported with LODs in the range

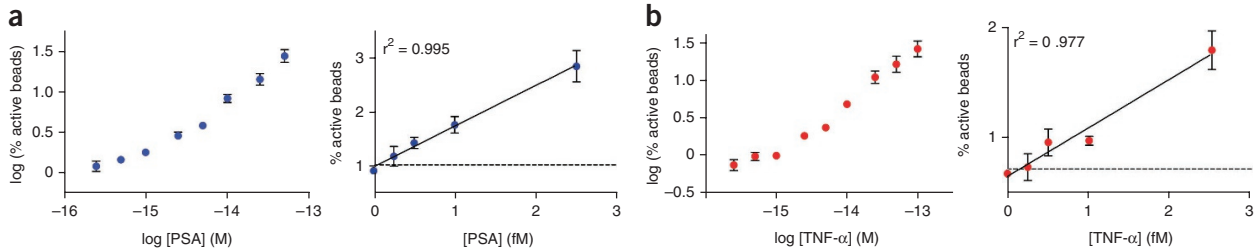
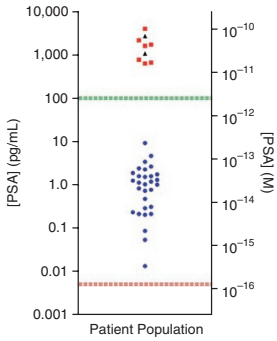


Figure 3 Subfemtomolar detection of proteins in serum using digital ELISA. (**a**,**b**) Changes in the percentage of active beads with changes in analyte concentration for human prostate-specific antigen (PSA) spiked into 25% serum (**a**) and human tumor necrosis factor-α (TNF-α) spiked into 25% serum (**b**). The concentrations plotted on the *x* axes refer to the final concentration of spiked protein in the diluted sample. The plots on the left-hand side show the assay response over the concentration range tested in log-log space. The plots on the right-hand side show the assay response in the femtomolar range in linear-linear space to illustrate the limit of detection (LODs) and linearity of response. LODs were determined by extrapolating the concentration from the signal equal to background signal plus 3 s.d. of the background signal. Broken lines, signal at the LOD. Error bars, s.d. over three replicates.

Fujirebio Diagnostics, Inc. v. Quanterix Corp.
EX-1005
000003



Patient ID	[PSA] (pg/mL)	Dose CV	Patient ID	[PSA] (pg/mL)	Dose CV	Patient ID	[PSA] (pg/mL)	Dose CV
S600	9.39	6%	S590	0.22	22%	S580	0.30	4%
S599	0.75	10%	S589	0.85	17%	S579	1.22	15%
S598	2.71	12%	S588	2.33	3%	S578	0.090	91%
S597	1.79	12%	S587	1.06	13%	S577	1.92	6%
S596	2.46	17%	S586	1.29	22%	S576	0.014	286%
S595	0.32	21%	S585	0.49	84%	S575	0.79	63%
S594	1.63	15%	S584	0.056	136%	S574	1.62	20%
S593	1.15	12%	S583	1.33	26%	S573	0.22	32%
S592	3.46	9%	S582	4.76	9%	S572	1.04	20%
S591	0.21	25%	S581	1.57	31%	S571	0.24	21%

Figure 4 Digital detection of prostate-specific antigen (PSA) in serum samples of patients who had undergone radical prostatectomy. Concentrations of PSA in serum samples from radical prostatectomy patients (●), healthy control samples (■) and Bio-Rad PSA control samples (▲) determined using digital ELISA. Radical prostatectomy patient samples (SeraCare Life Sciences) all had undetectable PSA levels as measured by a leading clinical diagnostic assay (ADVIA Centaur); the green broken line represents the detection limit of the ADVIA Centaur PSA assay (100 pg/ml or 3 pM). All 30 patient samples were above the detection limit of the PSA digital ELISA, shown by the red broken line (0.006 pg/ml or ~200 aM), with the lowest patient PSA concentrations measured at 0.014 pg/ml (~400 aM) using digital ELISA. Patient samples with the lowest PSA levels approached the LOD of the assay, resulting in a large imprecision in the concentration determined (high dose %CV). The digital ELISA was validated for specificity to PSA using control standards (Bio-Rad) and serum from healthy individuals (ProMedDx) that had been assayed using the ADVIA Centaur PSA assay (**Supplementary Table 3**).

© 2010 Nature America, Inc. All rights reserved.

of 10–30 fM[17,26]. The detection limit determined from the TNF-α digital ELISA was ~150 aM (2.5 fg/ml), corresponding to ~600 aM (10 fg/ml) in whole serum; the highest sensitivity commercially available ELISA for TNF-α has an LOD of 21 fM (0.34 pg/ml) in serum (**Supplementary Fig. 3**). The zero concentration spike of target protein for both assays provides a useful negative control for these experiments: 25% serum contains millimolar concentrations of a wide variety of proteins, and very low concentrations of target protein can be detected above these high-protein backgrounds. We also developed a proof-of-principle digital assay for DNA to show that low concentrations of nucleic acids can be detected without replication of the target (**Supplementary Fig. 2**).

The ability of digital ELISA to measure much lower concentrations of proteins than conventional ELISA derives from two effects: (i) the high sensitivity of SiMoAs to enzyme label and (ii) the low background signals that can be achieved by digitizing the detection of proteins. The sensitivity of any immunoassay is determined by the sensitivity of the detection technology to the label, the antibody affinity, the assay background and the variance (%CV) of the background measurement[27]. The subattomolar sensitivity of SiMoAs to enzyme labels (**Fig. 2**) enables digital ELISA to detect subfemtomolar concentrations of labeled proteins. That said, for antibodies of given affinity, the sensitivity of the immunoassay will be determined by the assay background, and the high label sensitivity of SiMoAs helps reduce this background. Control experiments have shown that backgrounds in digital ELISA arise from nonspecific binding of detection antibody and enzyme conjugate to the capture bead surface (**Supplementary Table 2**). As SiMoAs provide superior label sensitivity over conventional assays, substantially less detection antibody (~1 nM) and enzyme conjugate (1–50 pM) are needed to detect binding events as compared with conventional assays (labeling reagent concentrations ~10 nM). The decreased label concentration reduces nonspecific binding to the capture surface, resulting in much lower background signals. For example, in the TNF-α and PSA digital ELISAs, the levels of nonspecific binding were equivalent to the signal produced by 1.8 fM and 1.2 fM of target protein, respectively (**Fig. 3**). The highest sensitivity commercial TNF-α assay has a level of nonspecific binding equivalent to 85 fM of TNF-α (**Supplementary Fig. 3**), which is 50 times more than we observe using digital ELISA. The ability to reduce backgrounds in digital ELISA by lowering the concentration of labeling reagents enables more sensitive immunoassays than are possible using conventional assays.

To demonstrate the possible diagnostic value of detecting very low concentrations of proteins in blood using digital ELISA, we measured PSA in serum samples from patients who had undergone radical prostatectomy. Levels of serum PSA are used both to screen for prostate cancer and to monitor recurrence of the disease in patients who have undergone radical prostatectomy[28]. After radical prostatectomy the vast majority of PSA is eliminated, and concentrations fall below the detection limit of standard commercial assays (3 pM or 0.1 ng/ml). Although regular monitoring of these patients for increases in PSA concentrations can detect recurrence of prostate cancer, several years may pass after surgery for biochemical recurrence to be detected by current immunoanalyzers. The ability to accurately quantify PSA levels in patients who have undergone prostatectomy at very low concentrations (<300 fM or 10 pg/ml) should provide early indication of recurrence if PSA levels increase[17,29]. **Figure 4** shows PSA concentrations measured using digital ELISA in the serum of 30 patients (age 60–89) who had undergone radical prostatectomy and whose blood was collected at least 6 weeks after surgery. The PSA concentrations in the sera of all 30 patients were below the detection limit of commercial assays. Whole-serum samples were diluted 1:4 in buffer and measured using the digital ELISA specific for PSA (**Fig. 3a**). PSA was successfully detected in all 30 patients using digital ELISA, with concentrations ranging from 14 fg/ml to 9.4 pg/ml, with an average of 1.5 pg/ml. Further clinical studies are required to establish the diagnostic benefit of measuring PSA at femtogram per milliliter amounts in patients following radical prostatectomy.

By isolating and detecting single immunocomplexes in arrays of femtoliter-volume wells, digital ELISA enables clinically important proteins in serum to be measured at subfemtomolar concentrations. We believe that the improvement in sensitivity shown by digital ELISA over previously reported approaches will translate into diagnostic benefits. For example, PSA concentrations in 9 of the 30 radical prostatectomy samples assayed in this work fell below the LOD of the previously highest sensitivity PSA assay based on nanoparticle labels[17]. An attractive feature of this approach is the ability to directly use reagents developed for standard ELISA for substantially more sensitive assays. We continue to improve the SiMoA technology in two key areas. First, based on the sensitivity to enzyme label (**Fig. 2**), it seems that the sensitivity of protein detection could be increased at least 100-fold if nonspecific interactions that cause background signals could be minimized. The ability to isolate and interrogate single molecules on individual beads provides avenues for distinguishing antibody-antigen

Fujirebio Diagnostics, Inc. v. Quanterix Corp.
EX-1005
000004

binding events from nonspecifically bound complexes. Second, we are simplifying the logistics of the assays. Even in its present form, however, we believe that digital ELISA has the potential to facilitate earlier diagnosis and treatment of disease.

METHODS

Methods and any associated references are available in the online version of the paper at http://www.nature.com/naturebiotechnology/.

Note: Supplementary information is available on the Nature Biotechnology website.

ACKNOWLEDGMENTS

The project described was supported by Award Number R43CA133987 from the National Cancer Institute.

AUTHOR CONTRIBUTIONS

D.M.R., C.W.K., D.R.F., D.R.W. and D.C.D. conceived the approach. D.R.F. built the imaging system. D.M.R., C.W.K., T.G.C., S.C.H., L.S., P.P.P., A.J.R., E.P.F., J.D.R. and G.K.P. conducted the experiments. T.P. wrote the image analysis software. L.C. prepared reagents. D.M.R. and D.C.D. wrote the manuscript. All authors were involved in designing experiments, reviewing and discussing data, and commenting on the manuscript.

COMPETING FINANCIAL INTERESTS

The authors declare competing financial interests: details accompany the full-text HTML version of the paper at http://www.nature.com/naturebiotechnology/.

Published online at http://www.nature.com/naturebiotechnology/.
Reprints and permissions information is available online at http://npg.nature.com/reprintsandpermissions/.

1. Tessler, L.A., Reifenberger, J.G. & Mitra, R.D. Protein quantification in complex mixtures by solid phase single-molecule counting. *Anal. Chem.* **81**, 7141–7148 (2009).
2. Todd, J. *et al.* Ultrasensitive flow-based immunoassays using single-molecule counting. *Clin. Chem.* **53**, 1990–1995 (2007).
3. Gosling, J.P.A. Decade of development in immunoassay methodology. *Clin. Chem.* **36**, 1408–1427 (1990).
4. Wild, D. *The Immunoassay Handbook 3rd Edn.* (Elsevier, 2005).
5. Zhang, H.Q., Zhao, Q., Li, X.F. & Le, X.C. Ultrasensitive assays for proteins. *Analyst (Lond.)* **132**, 724–737 (2007).
6. Giljohann, D.A. & Mirkin, C.A. Drivers of biodiagnostic development. *Nature* **462**, 461–464 (2009).
7. Srinivas, P.R., Kramer, B.S. & Srivastava, S. Trends in biomarker research for cancer detection. *Lancet Oncol.* **2**, 698–704 (2001).
8. Galasko, D. Biomarkers for Alzheimer's disease—clinical needs and application. *J. Alzheimers Dis.* **8**, 339–346 (2005).
9. de Jong, D., Kremer, B.P.H., Olde Rikkert, M.G.M. & Verbeek, M.M. Current state and future directions of neurochemical biomarkers for Alzheimer's disease. *Clin. Chem. Lab. Med.* **45**, 1421–1434 (2007).
10. Barletta, J.M., Edelman, D.C. & Constantine, N.T. Lowering the detection limits of HIV-1 viral load using real-time immuno-PCR for HIV-1 p24 antigen. *Am. J. Clin. Pathol.* **122**, 20–27 (2004).
11. Adler, M., Wacker, R. & Niemeyer, C.M. Sensitivity by combination: immuno-PCR and related technologies. *Analyst (Lond.)* **133**, 702–718 (2008).
12. Nam, J.M., Thaxton, C.S. & Mirkin, C.A. Nanoparticle-based bio-bar codes for the ultrasensitive detection of proteins. *Science* **301**, 1884–1886 (2003).
13. Armani, A.M., Kulkarni, R.P., Fraser, S.E., Flagan, R.C. & Vahala, K.J. Label-free, single-molecule detection with optical microcavities. *Science* **317**, 783–787 (2007).
14. Cui, Y., Wei, Q.Q., Park, H.K. & Lieber, C.M. Nanowire nanosensors for highly sensitive and selective detection of biological and chemical species. *Science* **293**, 1289–1292 (2001).
15. Gaster, R.S. *et al.* Matrix-insensitive protein assays push the limits of biosensors in medicine. *Nat. Med.* **15**, 1327–1332 (2009).
16. Fan, R. *et al.* Integrated barcode chips for rapid, multiplexed analysis of proteins in microliter quantities of blood. *Nat. Biotechnol.* **26**, 1373–1378 (2008).
17. Thaxton, C.S. *et al.* Nanoparticle-based bio-barcode assay redefines "undetectable" PSA and biochemical recurrence after radical prostatectomy. *Proc. Natl. Acad. Sci. USA* **106**, 18437–18442 (2009).
18. Bao, Y.P. *et al.* Detection of protein analytes via nanoparticle-based bio bar code technology. *Anal. Chem.* **78**, 2055–2059 (2006).
19. Anderson, N.L. & Anderson, N.G. The human plasma proteome: history, character, and diagnostic prospects. *Mol. Cell. Proteomics* **1**, 845–867 (2002).
20. Gorris, H.H., Rissin, D.M. & Walt, D.R. Stochastic inhibitor release and binding from single-enzyme molecules. *Proc. Natl. Acad. Sci. USA* **104**, 17680–17685 (2007).
21. Rissin, D.M., Gorris, H.H. & Walt, D.R. Distinct and long-lived activity states of single enzyme molecules. *J. Am. Chem. Soc.* **130**, 5349–5353 (2008).
22. Rissin, D.M. & Walt, D.R. Digital readout of target binding with attomole detection limits via enzyme amplification in femtoliter arrays. *J. Am. Chem. Soc.* **128**, 6286–6287 (2006).
23. Rissin, D.M. & Walt, D.R. Digital concentration readout of single enzyme molecules using femtoliter arrays and Poisson statistics. *Nano Lett.* **6**, 520–523 (2006).
24. Tan, W. & Yeung, E.S. Monitoring the reactions of single enzyme molecules and single metal ions. *Anal. Chem.* **69**, 4242–4248 (1997).
25. Rissin, D.M. & Walt, D.R. Duplexed sandwich immunoassays on a fiber-optic microarray. *Anal. Chim. Acta* **564**, 34–39 (2006).
26. Ferguson, R., Yu, H., Kalyvas, M., Zammit, S. & Diamandis, E. Ultrasensitive detection of prostate-specific antigen by a time-resolved immunofluorometric assay and the Immulite immunochemiluminescent third-generation assay: potential applications in prostate and breast cancers. *Clin. Chem.* **42**, 675–684 (1996).
27. Jackson, T.M. & Ekins, R.P. Theoretical limitations on immunoassay sensitivity. Current practice and potential advantages of fluorescent Eu^{3+} chelates as non-radioisotopic tracers. *J. Immunol. Methods* **87**, 13–20 (1986).
28. Bock, J.L. & Klee, G.G. How sensitive is a prostate-specific antigen measurement? How sensitive does it need to be? *Arch. Pathol. Lab. Med.* **128**, 341–343 (2004).
29. Trock, B.J. *et al.* Prostate cancer-specific survival following salvage radiotherapy vs observation in men with biochemical recurrence after radical prostatectomy. *Jama-Journal of the American Medical Association* **299**, 2760–2769 (2008).

© 2010 Nature America, Inc. All rights reserved.

Fujirebio Diagnostics, Inc. v. Quanterix Corp.
EX-1005
000005

ONLINE METHODS

Materials. Optical fiber bundles were purchased from Schott North America. Nonreinforced gloss silicone sheeting was obtained from Specialty Manufacturing. Hydrochloric acid, anhydrous ethanol and molecular biology–grade Tween-20 were all from Sigma-Aldrich. Carboxyl-terminated magnetic beads (2.7-μm diameter) were purchased from Varian. Monoclonal capture antibody to human TNF-α, polyclonal detection antibody to human TNF-α and recombinant human TNF-α were purchased from R&D Systems. Monoclonal capture antibody to PSA, monoclonal detection antibody to PSA and purified PSA were purchased from BiosPacific; the detection antibody was biotinylated using standard methods. 1-ethyl-3-(3-dimethylaminopropyl) carbodiimide hydrochloride, N-hydroxysulfosuccinimide and SuperBlock T-20 Blocking Buffer were purchased from Thermo Scientific. Purified DNA was purchased from Integrated DNA Technologies. SβG was conjugated in the laboratory using standard protocols. RGP was purchased from Invitrogen. The fiber polisher and polishing consumables were purchased from Allied High Tech Products.

Preparation of magnetic beads presenting biotin-labeled DNA and capture of enzyme conjugate (Fig. 2). Beads functionalized with DNA capture probe (5′-NH_2/C12-GTT GTC AAG ATG CTA CCG TTC AGA G-3′) were prepared according to the manufacturer's instructions. These beads were incubated with 1 μM of biotinylated complementary DNA (5′-biotin-C TCT GAA CGG TAG CAT CTT GAC AAC-3′) overnight (16 h) in TE buffer containing 0.5 M NaCl and 0.01% Tween-20. After incubation the beads were washed three times in PBS buffer containing 0.1% Tween-20. The bead stock was distributed into a microtiter plate giving 400,000 beads per well in 100 μl. The buffer was aspirated from the microtiter plate wells; the beads were resuspended and incubated with various concentrations of SβG in Superblock containing 0.05% Tween-20 for 4 h. The beads were then separated and washed six times with 5× PBS buffer containing 0.1% Tween-20. For detection of enzyme, the beads were either (i) resuspended in 20 μl of PBS containing 0.1% Tween-20, and 10-μl aliquots were loaded onto two femtoliter-volume well arrays for SiMoA detection; or (ii) resuspended in 100 μl of 100 μM RGP in PBS, incubated for 1 h at 23 °C and read on a fluorescence plate reader (Infinite M200, Tecan).

Capture of proteins on magnetic beads and formation of enzyme-labeled immunocomplex (Figs. 3 and 4). Beads functionalized with an antibody to the target protein were prepared according to the manufacturer's instructions. Test solutions (100 μl) containing the protein of interest were incubated with suspensions of 200,000 magnetic beads for 2 h at 23 °C. The beads were then separated and washed three times in PBS and 0.1% Tween-20. The beads were resuspended and incubated with solutions containing detection antibody (typically ~1 nM) for 45 min at 23 °C. The beads were then separated and washed three times in PBS and 0.1% Tween-20. The beads were incubated with solutions containing SβG (1–50 pM) for 30 min at 23 °C, separated and washed six times in PBS and 0.1% Tween-20. The beads were then resuspended in 10 μl of PBS and loaded onto a femtoliter-volume well array. The total time of the assay was ~6 h.

Capture of DNA on magnetic beads and formation of enzyme-labeled complex (Supplementary Fig. 2). A total of 200,000 beads functionalized with DNA capture probe were incubated with 100-μl solutions containing the target DNA (5′-TT GAC GGC GAA GAC CTG GAT GTA TTG CTC C TCT GAA CGG TAG CAT CTT GAC AAC-3′) for 2 h. After incubation, the DNA target solution was removed and the beads were washed three times in 0.2× SSC buffer containing 0.1% Tween-20. The beads were then resuspended and mixed with 10 nM biotinylated signal probe (5′-TAC ATC CAG GTC TTC GCC GTC AA/Biotin/-3′) that is also specific to the target DNA for 1 h. The beads were then washed three times in 0.2× SSC buffer containing 0.1% Tween-20 after removing the signal probe. A solution of 10 pM SβG was then added to the bead pellet, resuspended and mixed for 1 h. The beads were separated and washed six times in 5× PBS buffer containing 0.1% Tween-20. The beads were then resuspended in 10 μl of PBS and loaded onto a femtoliter-volume well array.

Preparation of femtoliter-volume well arrays. Optical fiber bundles approximately 5 cm long were sequentially polished on a polishing machine using 30-, 9- and 1-μm-sized diamond lapping films. The polished fiber bundles were chemically etched in a 0.025 M HCl solution for 130 s and then immediately submerged into water to quench the reaction. The etched fibers were sonicated for 5 s in water, washed in water for 5 min and dried under vacuum. The differential etch rate of the core and cladding glass of the fiber bundle arrays caused 4.5-μm-diameter wells to be formed in the core fibers[30]. Different etch times resulting in different well depths were initially investigated. If wells were too deep, then multiple beads were deposited in each well and sealing was disrupted; if wells were too shallow, then the beads were not retained in the wells and poor loading efficiencies were observed. Well depths of 3.25 ± 0.5 μm were optimal for retaining single beads in wells while maintaining good seals.

Loading of beads into femtoliter-volume well arrays. A short length of PVC tubing was placed on the etched end of a fiber bundle to create a reservoir to hold the bead solution. Ten microliters of the concentrated bead solution were pipetted into this reservoir. The fiber bundle was then centrifuged at 1,300*g* for 10 min to force the beads into the etched wells. The PVC tubing was removed after centrifugation. The fiber bundle was dipped in PBS solution to wash off excess bead solution, and the surface was swabbed with deionized water. In addition to well depth (see above), bead concentration was an important parameter for maximizing bead loading efficiencies. Above concentrations of 200,000 beads per 10 μl loaded, typically 40–60% of wells in a 50,000-well array were occupied by a single bead, resulting in percentage active beads with acceptable Poisson noise. At concentrations below 200,000 beads per 10 μl loaded, bead loading efficiency dropped, resulting in fewer active beads and higher Poisson noise. In these experiments, therefore, at least 200,000 beads per reaction were used and loaded onto the arrays.

Detection of beads and enzyme-labeled beads in femtoliter-volume well arrays. A custom-built imaging system containing a mercury light source, filter cubes, objectives and a CCD camera was used for acquiring fluorescence images[21,23]. Fiber bundles were mounted on the microscope stage using a custom fixture. A droplet of β-galactosidase substrate (RGP) was placed on the silicone gasket material and placed in contact with the well arrays. A precision mechanical platform moved the silicone sheet into contact with the end of the fiber bundle, creating an array of isolated femtoliter-volume reaction vessels. Fluorescence images were acquired (558 nm excitation; 577 nm emission) with an exposure time of 1,011 ms. Five frames (at 30-s intervals) were taken for each femtoliter-volume well array. The product of the enzymatic reaction used in these studies—resorufin—has high photostability with a low photobleaching rate (rate of photobleaching, $k_{ph} = 0.0013\ s^{-1}$)[21], making multiple exposures possible. We performed time-course fluorescence measurements (i) to allow stable fluorescent artifacts to be removed from images and (ii) to ensure that the signal from a beaded well was from an enzyme. For (i), the first fluorescent image was subtracted from fluorescent images acquired at each subsequent time point. This process removed light intensity that did not change with time; for example, fluorescence from dust and scattered light. For (ii), a positive or "on" well was identified only where fluorescence intensity in a beaded well increased in every frame and by at least 20% over four frames. This process removed false positives from random changes in fluorescence during image acquisition. **Supplementary Figure 1** shows histograms of fluorescence from wells with and without enzymes, showing the good distinction between "on" and "off" wells. Arrays were also imaged with white light to identify those wells that contain beads. After acquiring the fluorescence images, the arrays were illuminated with white light and imaged on the CCD camera. Due to scattering of light by the beads, those wells that contained a bead appeared brighter in the image than wells without beads. The fluorescence and white-light images were analyzed using customized software.

30. Pantano, P. & Walt, D.R. Ordered nanowell arrays. *Chem. Mater.* **8**, 2832–2835 (1996).

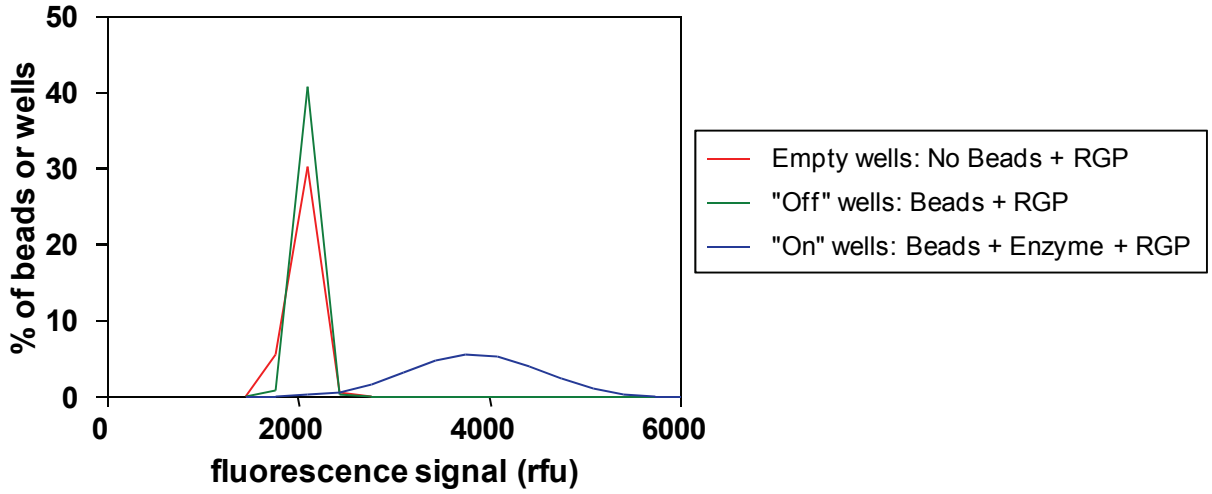
© 2010 Nature America, Inc. All rights reserved.

doi:10.1038/nbt.1641

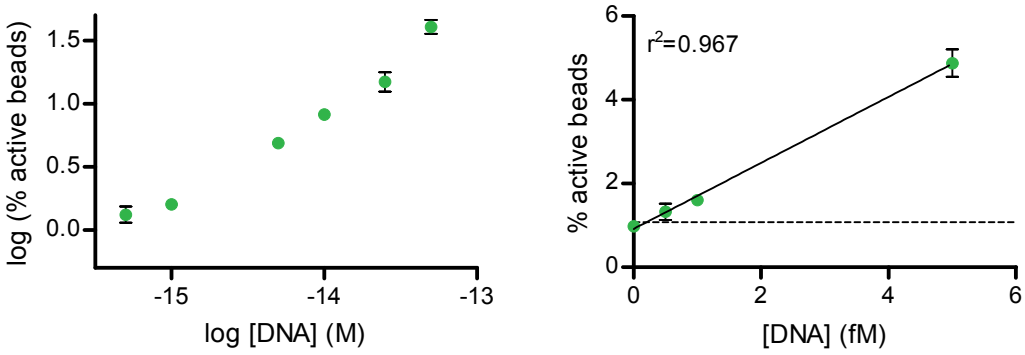
Fujirebio Diagnostics, Inc. v. Quanterix Corp.
EX-1005
000006

Supplementary Information

1) Supplementary Figures and Legends



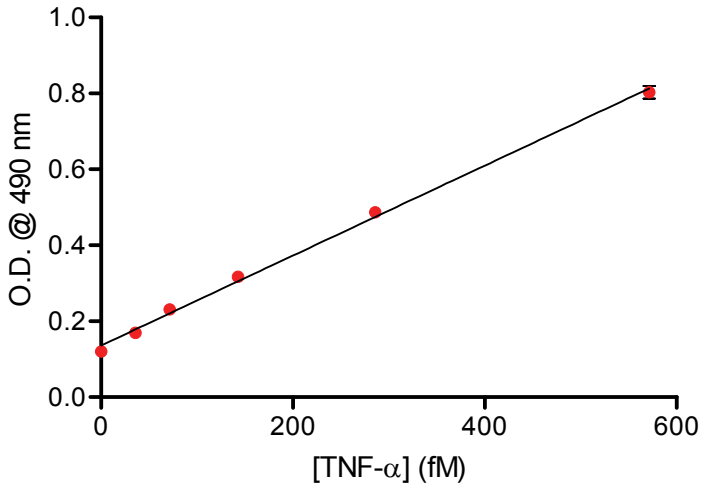
Supplementary Figure 1. Histograms of the average fluorescence intensity of wells in a SiMoA experiment. A representative set of images from a SiMoA experiment (Figure 1) were analyzed to determine populations of wells that: a) contained no beads; b) contained a bead (from white light scatter) but no enzyme (no increase in fluorescence intensity); and, c) contained a bead (from white light scatter) and an enzyme (increasing fluorescence intensity over four consecutive images, and an overall increase in fluorescence of at least 20%). Using this method of calling "on" wells, the occurrence of false positives in the absence of background proteins is very small (<1 in a 50,000-well array, see Figure 2). In the presence of background proteins, e.g., serum samples, there is a significant number of "on" wells from non-specific binding that sets the background signal and limits of detection (see discussion in main text). The fraction of beads within each population is plotted against the average intensity of wells with a bin size of 120 rfu. The red line represents data from empty wells; the green line represents wells with a bead but no enzyme ("off" well); and the blue line represents beads with both a bead and enzymatic activity ("on" well). While a range of enzyme activities are observed as anticipated[21], there is good separation between on and off wells to allow digital quantification.



Supplementary Figure 2. Detection of DNA using digital counting of enzyme labels. Plots of % active beads against different concentrations of DNA spiked into buffer. Experimental details are provided in the Methods section. The plot on the left hand side show the assay response over the

Nature Biotechnology: doi: 10.1038/nbt.1641

concentration range tested in log-log space. The plot on the right hand side show the assay response in the femtomolar range in linear-linear space. Error bars are plotted as the standard deviation over three replicates. LODs were determined by extrapolating the concentration from the signal equal to background signal plus three standard deviations of the background signal; the dashed lines show the signal at the LOD. The LOD of the digital DNA sandwich assay was ~150 aM, corresponding to about 8000 copies. While these results are preliminary—the DNA was detected in buffer in the absence of non-target DNA—and the sensitivity does not approach that that can be achieved with PCR, they do illustrate that SiMoA can be used to detect nucleic acids without recourse to molecular replication.



Supplementary Figure 3. The R&D Systems HS-ELISA for TNF-α. A TNF-α calibration curve yielded an LOD of 21 fM in whole serum using a Tecan Infinite M200 plate reader. The non-specific binding (NSB) background in this high sensitivity assay was equivalent to about 85 fM of TNF-α.

2) Supplementary Tables

	Column A	Column B	Column C	Column D	Column E	Column F
[SβG] (aM)	Average % active beads observed (Figure 2)	Enzyme/bead ratio from Poisson distribution	Total # of enzymes on 400,000 beads	Background corrected # of enzymes on beads	Calculated # of enzymes in 100-µL sample	Capture Efficiency
0	0.0016%	0.000016	7	---	---	---
0.35	0.0086%	0.000086	34	28	21	132%
0.7	0.0099%	0.000099	40	33	42	79%
3.5	0.0413%	0.000413	165	159	211	75%
7	0.0713%	0.000713	285	279	421	66%
35	0.4461%	0.004471	1789	1782	2107	85%
70	0.8183%	0.008217	3287	3280	4214	78%
350	3.3802%	0.034387	13755	13748	21070	65%
700	7.5865%	0.078897	31559	31552	42140	75%
3500	30.6479%	0.365974	146390	146383	210700	69%
7000	44.5296%	0.589320	235728	235722	421400	56%

Nature Biotechnology: doi: 10.1038/nbt.1641

Fujirebio Diagnostics, Inc. v. Quanterix Corp.
EX-1005
000008

Supplementary Table 1. Calculations of the SiMoA capture efficiency of enzyme label from 0.35 aM to 7000 aM. From the fraction of beads that were active in Figure 2 (Column A), the enzyme/bead ratio (Column B) can be determined from the Poisson distribution[23]. In this experiment, ~400,000 beads were incubated with each solution of enzyme (although only ~50,000 beads (~12.5%) on average were interrogated because of the current size of the femtoliter arrays (~50,000 wells)), so the number of enzymes on these beads is determined by multiplying Column B by 400,000 (Column C). After background subtraction, the total number of enzyme molecules captured on the beads can be determined (Column D). The ratio of this number to the total calculated number of enzymes in 100 μL at the start of the experiment (Column E; Volume × Concentration × Avogadro's Number) yields a capture efficiency (Column F). The overall efficiency of capture and detection of enzyme using SiMoA is high (65-85%) in the range where Poisson noise is acceptable (<20%, from 3.5 aM to 3500 aM), and is probably only limited in this experiment by the slow diffusion of the large SβG conjugate (MW ~ 515 kDa). At 7000 aM, where the % active beads > 40%, the % active starts to deviate from linearity (giving rise to an apparent lower capture efficiency) because of difficulties in image analysis at these high fractions (see main text).

NSB Dropout Experiment (SiMoA PSA assay)					
	Average	SD	CV	% NSB	
No dAb; No PSA	0.110%	0.162%	147%	from SbG	20%
No SbG; No PSA	0.000%	0.000%	---	from dAb	80%
NSB	0.541%	0.194%	36%	Total NSB	100%

Supplementary Table 2. A dropout experiment isolating the sources of NSB in the PSA digital ELISA. By comparing 'no detection antibody NSB' (No dAb) and 'no SβG NSB' (No SβG) to total NSB (NSB), the contribution of detection antibody and SβG to the NSB of the assay was determined.

	Centaur ng/mL	**SiMoA ng/mL**
Bio-Rad Control 1	0.838	1.06 ± 0.21
Bio-Rad Control 2	2.47	2.66 ± 0.36
Normals		
ProMedDx S376	2.1	1.60
ProMedDx S378	2.3	1.70
ProMedDx S381	2.9	2.14
ProMedDx S388	4.1	3.95
ProMedDx S395	0.93	0.63
ProMedDx S396	0.9	0.77
ProMedDx S397	1.2	0.66

Supplemental Table 3. Specificity of the PSA digital ELISA. Specificity of the digital ELISA was confirmed using PSA samples from Bio-Rad (controls) and ProMedDx (serum from healthy individuals) that had previously been tested on a commercial immunoanalyzer (ADVIA Centaur, Siemens). While there was good correlation between the two methods (r^2 = 0.96), the PSA concentrations of the healthy

Nature Biotechnology: doi: 10.1038/nbt.1641

serum samples determined using SiMoA were (24±12)% lower than those originally determined on the ADVIA Centaur. There are two possible explanations for this systematic bias between the two technologies. First, the ADVIA Centaur values were obtained on fresh serum, whereas digital ELISA values were obtained after the sera had been frozen for extended periods of time and had experienced a freeze-thaw cycle. Second, there were likely differences between the PSA calibrators used to generate the calibration curves that would result in differences in PSA concentrations determined. We used Complex PSA from the World Health Organization (WHO) as calibrators; the ADVIA Centaur calibration PSA is unknown.

3) Supplementary Discussion

Sensitivity to Enzyme Label as Sample Volume Increases. For some applications, volumes larger than 100 μL might need to be tested for very low concentrations of analyte. As the volume of sample increases, detecting small numbers of enzyme labels with high efficiency becomes more challenging technically. To achieve the same detection efficiencies in 1 mL and 10 mL of sample that we achieved in 100 μL, would require 10 and 100 times more beads, respectively, both from thermodynamic and kinetic perspectives. These larger numbers of beads (2 million and 20 million) would require much bigger arrays and also larger imaging (CCD) chips or multiple images per array. While these experiments are feasible, they would require a much more complex instrument and longer read times, so might not be justified in a diagnostic setting.

Optimization of Labeling of Captured Proteins in Digital ELISA. The choice of the concentrations of detection antibody and enzyme conjugate (SβG) used to label the captured protein is important for optimizing digital ELISA. The relatively high background signals of ELISAs caused by the non-specific interactions between the capture beads and detection antibody and enzyme conjugate (see Supplementary Table 2), combined with the high sensitivity to label provided by SiMoA, means that often only a fraction of the capture proteins need to be labeled to avoid saturating SiMoA signals. For example, the background levels observed in digital ELISA are equivalent to ~1–2 fM of target protein (see main text), so the ratio of analyte to bead is about 0.3–0.6. At these ratios, the number of active beads would be 25–40% if every protein was labeled with an enzyme, i.e., at the upper end of the digital dynamic range. To ensure that these background signals are closer to the lower end of the digital dynamic range—1% active beads provides a reasonable noise floor for background in digital ELISA—appropriate labeling of the captured protein can be achieved by kinetic control of the labeling steps, either by minimizing the concentrations of both labeling reagents or by using shorter incubation times. We have chosen to minimize label concentrations and use standard ELISA incubation times; as a result, the total assay time is ~6 h. This length of time is acceptable for testing that tolerates a daily turnaround time for samples. For shorter turnaround times of, say, <1 h (e.g., for point-of-care applications), the assay could be performed with short incubations of higher concentrations of labeling reagents.

Nature Biotechnology: doi: 10.1038/nbt.1641